

Supporting Information

Singlet oxygen is not the source of ethylene carbonate degradation in nickel-rich Li-ion cells

Rory C. McNulty,^{abcd†} Kieran D. Jones,^{abcd†} Benjamin M. G. Denison,^{abcd} Elizabeth Hampson,^{abc} Israel Temprano,^{ef} Darren A. Walsh,^{abcd} Hon Wai Lam,^{bc} Graham N. Newton,^{abcd} Wesley M. Dose,^{dg} Clare P. Grey,^{de} Lee R. Johnson^{*abcd}

^aNottingham Applied Materials and Interfaces Group, School of Chemistry, University of Nottingham, NG7 2TU, UK

^bThe GSK Carbon Neutral Laboratories for Sustainable Chemistry, University of Nottingham, Jubilee Campus, Triumph Road, Nottingham, NG7 2TU, UK

^cSchool of Chemistry, University of Nottingham, University Park, Nottingham, NG7 2RD, UK

^dThe Faraday Institution, Quad One, Harwell Science and Innovation Campus, Didcot, OX11 0RA, UK

^eYusuf Hamied Department of Chemistry, University of Cambridge, Lensfield Road, Cambridge, CB2 1EW, UK

^fCICA - Interdisciplinary Center for Chemistry and Biology, University of A Coruña, 15071, A Coruña, Spain

^gSchool of Chemistry, University of Sydney, Camperdown, NSW, 2006, Australia

[†] These authors contributed equally to this work

*lee.johnson@nottingham.ac.uk

Contents

General Information	2
Experimental	3
Cell configuration & cycling.....	3
Linear sweep voltammetry	3
Detection of vinylene carbonate by gas chromatography mass spectrometry.....	3
On-line Mass-Spectrometry Analysis.....	5
Supplementary note 1 – Long-term cycling at an UCV greater than 4.2 V.....	6
Supplementary Note 2 – Extended exposure study of EC to ¹ O ₂	14
References	16

General Information

Reagents and solvents. Ethylene carbonate (EC, 98%), 9,10-dimethylantracene (DMA, 99%), 4,5,6,7-tetrachloro-2',4',5',7'-tetraiodofluorescein disodium salt (rose bengal, RB), and 5,10,15,20-Tetraphenyl-21*H*,23*H*-porphine (TPP) were purchased from Sigma-Aldrich and used without further purification. Deuterated chloroform (CDCl_3 , 99.8% D), deuterated dimethyl sulfoxide (d_6 -DMSO, 99.9% D) were purchased from Sigma Aldrich.

Electrochemical materials. $\text{LiNi}_{0.8}\text{Mn}_{0.1}\text{Co}_{0.1}\text{O}_2$ (NMC811) (8.21 mg cm^{-2} , 1.52 mAh cm^{-2}), $\text{LiNi}_{0.33}\text{Mn}_{0.33}\text{Co}_{0.33}\text{O}_2$ (NMC111) (10.10 mg cm^{-2} , 1.48 mAh cm^{-2}), and graphite (Gr) (5.83 mg cm^{-2} , 2.09 mAh cm^{-2}) electrodes were supplied by the U.S. Department of Energy's CAMP Facility, Argonne National Laboratory. NMC811 and NMC111 electrodes comprised 90% active material, 5% conductive carbon support, and 5% binder coated on aluminium foil. The base electrolyte (LP57, 1 M LiPF_6 in ethylene carbonate (EC): ethyl methyl carbonate (EMC) = 3:7 v/v) and the formulated electrolyte with 2 wt.% vinylene carbonate (VC) additive were purchased from Solvionic (99.9%, $\text{H}_2\text{O} \leq 20 \text{ ppm}$). NMC811, NMC111, and Gr electrodes were dried under vacuum at $120 \text{ }^\circ\text{C}$ for 24 hours before being transferred into an Ar-filled glovebox (MBraun, O_2 and $\text{H}_2\text{O} \leq 0.1 \text{ ppm}$) without exposure to air. Model electrolyte solutions were prepared by mixing ethylene carbonate (99%, Sigma Aldrich) with ethyl methyl carbonate (99%, Sigma Aldrich) in a 3:7 v/v ratio in an N_2 -filled glovebox (MBraun, O_2 and $\text{H}_2\text{O} \leq 0.1 \text{ ppm}$).

Nuclear magnetic resonance (NMR) spectroscopy details. ^1H NMR spectroscopy was acquired on a Bruker AV(III)500 HD fitted with a 5 mm prodigy BBO cryoprobe. Respective deuterated solvents were used as the lock solvents. The internal references trimethoxy benzene and dimethyl sulfone were purchased from Sigma-Aldrich and used without further purification. The chemical shifts in ^1H spectra were referenced to the residual (partially) non-deuterated solvent according to Fulmer et al.¹

Photochemical details. Kessil H160 Tuna Flora lamp (40W) in red mode at 100% intensity, or green LED bulb (5 W, 500 lm) were used. Emission spectra were measured using an Ocean Optics spectrometer (USB2000+UV-VIS-ES) recorded on SpectroLab software (**Figure S1**). Lamps were positioned with bulb-to-vial distances ca. 10 mm during the reactions.

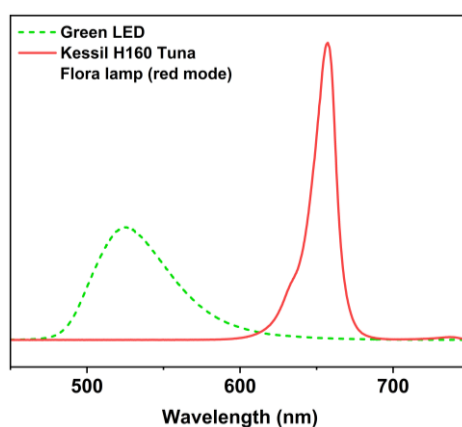


Figure S1. Emission spectra of Kessil H160 Tuna Flora lamp (red mode) and green LED.

Experimental

Cell configuration & cycling

Cells were assembled inside an Ar-filled glovebox. All measurements were carried out at 20 °C with an initial equilibration time of 1-hour allowed for electrode wetting and temperature uniformity. Long-term cycling experiments used a Celgard (2032) separator soaked in 80 μL of electrolyte, and VC detection cells employed Whatman glass microfiber filter paper (GF/F) as the separator, with 120 μL of electrolyte. Cells were cycled using a two-electrode Swagelok cell, pairing 12 mm electrodes. C-rates were calculated assuming a nominal NMC811 capacity of 190 $\text{mAh g}^{-1}_{\text{NMC}}$. Battery cycling was carried out on an IviCycle200 potentiostat.

Linear sweep voltammetry

Linear sweep voltammetry was carried out in a three neck round bottom flask in an Ar filled glovebox (<0.5 ppm O_2 <0.5 ppm H_2O). The experiments were performed on a Biologic SP300 potentiostat, with manual IR correction at a scan rate of 50 mVs^{-1} . All experiments used a glassy carbon working electrode, platinum counter electrode, and lithium metal reference electrode submerged in 3 mL of electrolyte.

Detection of vinylene carbonate by gas chromatography mass spectrometry

Two cycling protocols were employed: i) three C/20 formation cycles to the desired UCV, ii) three C/20 formation cycles to the specified UCV and then an additional ten cycles at C/2 to that UCV. All cells were cycled with VC-free LP57 electrolyte. After cycling (for capacities see **Figure S2**), cells were disassembled in an Ar-filled glovebox and the glass microfiber filter paper was soaked in 1.5 mL CDCl_3 for 30 minutes.² GC-MS samples were injected into the inlet with a split-less flow at 200 °C and carried onto the preheated column which was held at 40 °C for 3 minutes. The oven temperature was then ramped at 2 °C min^{-1} for 10 minutes to a final temperature of 60 °C. The MS transfer line and ion source were held at 250 °C, and the MS transfer line was opened after 8 minutes. VC was identified at a retention time of *ca.* 9.7 minutes under these conditions to a high degree of confidence through comparison of experimental MS data to the NIST mass spectral library (**Figure S3**).³

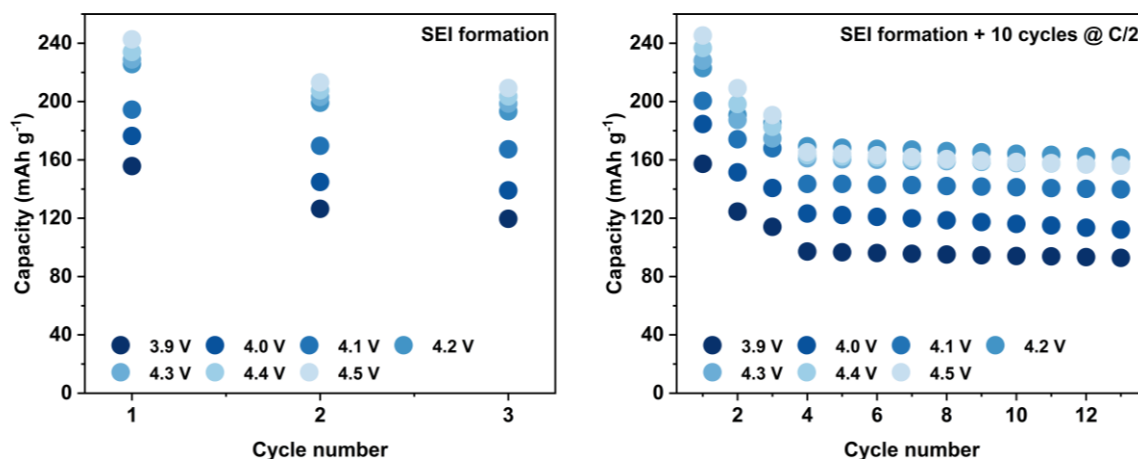


Figure S2. Capacities of Gr-NMC811 full-cells cells used for *ex situ* detection of VC by GCMS shown in **Figure 2**.

To improve instrument sensitivity, the detector mass range was limited to 40 – 100 amu, and an 86 amu restriction was applied to the data to reduce background noise. The limit of quantification (LOQ) was defined as the concentration at which quantitative analysis can be reported with a high degree of confidence, determined by recording the mean value of the noise of a blank sample plus 10× the standard deviation of the noise.⁴ The LOQ of VC was determined to be *ca.* 135 ppb.

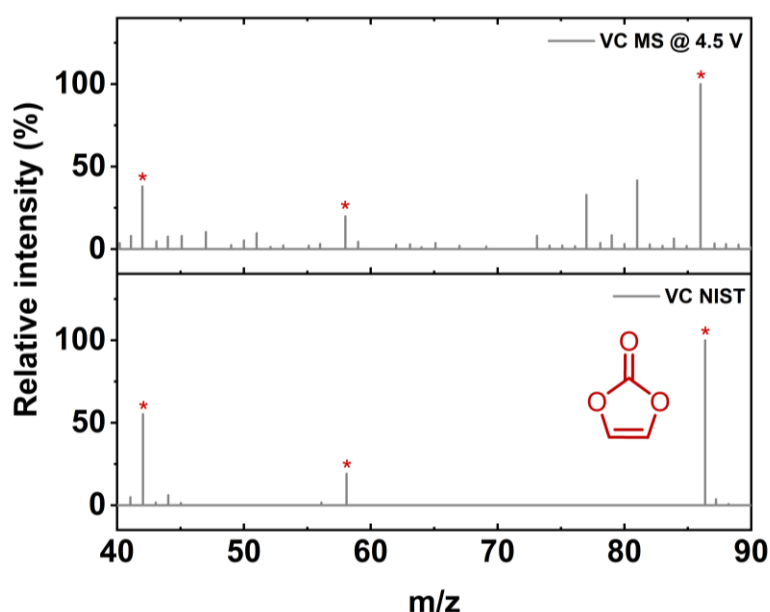


Figure S3. Example mass spectrum (electron impact ionisation) of chromatography peak corresponding to VC from *ex situ* collection vs NIST data base.

A Gr-Ni_{0.33} Mn_{0.33} Co_{0.33} O₂ (NMC111) full-cell was cycled according to regime **ii** to an UCV of 4.3 V, the cell was disassembled and subjected to the GC-MS protocol as described above. VC was detected by GC-MS (**Figure S4**).

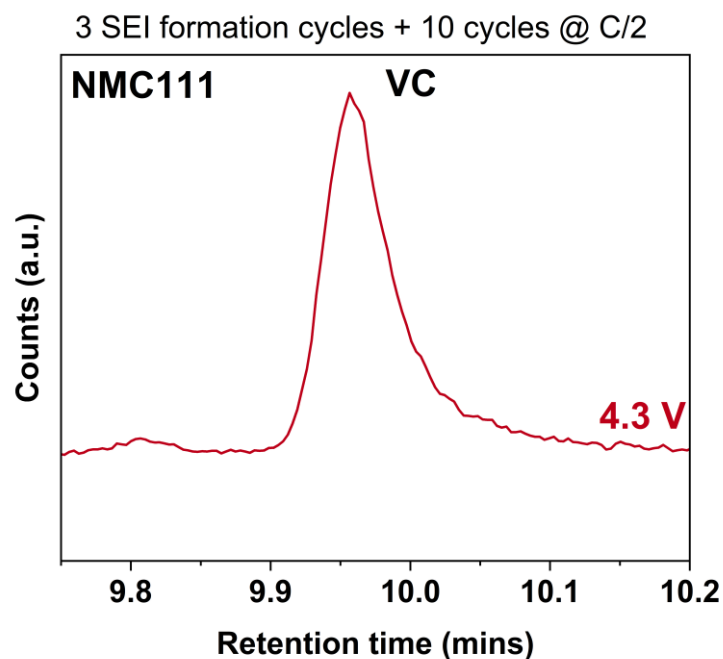


Figure S4. GC-MS plot of the electrolyte of a Gr-NMC111 full cell cycled to an UCV of 4.3 V for 3 × C/20 formation cycles and 10 cycles at C/2.

On-line Mass-Spectrometry Analysis

Online electrochemical mass spectrometry (OEMS). OEMS measurements were performed on a Li-NMC811 half-cell pairing an 18 mm NMC811 positive electrode with a 15.6 mm metallic lithium counter/reference electrode, with glass fibre separators soaked in 300 μ L of electrolyte. The cell was controlled with an Ivium potentiostat and charged to an UCV of 4.6 V at a rate of C/20, where a 40-hour voltage hold period was performed, before being discharged to 2.5 V vs Li⁺|Li. The OEMS system consisted of a stainless-steel tube which carried gas through the electrochemical cell, connected through self-sealing quick-connects (Beswick Engineering) to a mass spectrometer, ensuring an air free system. Ar (N6.0, BOC) carrier gas was used, connected to a gas purifier before flow control. A quadrupole mass spectrometer (Pfeiffer) was connected to the cell through a heated capillary (120 °C) to prevent condensation of volatile species. O₂ gas evolution was calculated by recording the intensity of the signal ($m/z = 32$) and converting to rate of gas evolution by calibration plot.

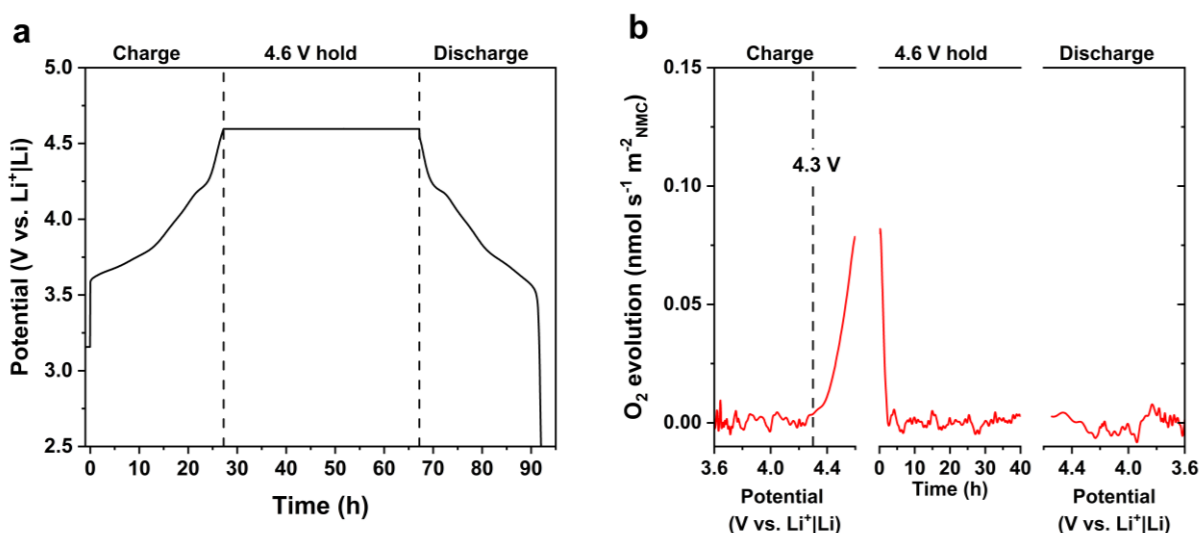


Figure S5. Full OEMS data where **a)** shows the potential of the NMC electrode during cycling, and **b)** the associated oxygen evolution.

Table S1. Conversion table for NMC811 potential vs. Li⁺|Li to UCV observed in a Gr-NMC811 full cells as seen in **Figure 2d**. Data obtained using a three-electrode cell consisting of an NMC811 cathode, Gr anode, and Li chip reference electrode.

UCV in full cell (V)	Potential vs. Li ⁺ Li (V)
3.9	3.99
4.0	4.08
4.1	4.18
4.2	4.28
4.3	4.38
4.4	4.48

Supplementary note 1 – Long-term cycling at an UCV greater than 4.2 V

In comparison to cells cycled to an upper cutoff voltage (UCV) of 4.2 V, an UCV of 4.4 V demonstrated greater capacity fade over 300 cycles (**Figure S6**). Cells containing 2 wt.% VC were also found to perform significantly worse than VC-free cells when cycled with an UCV of 4.4 V comparatively to that of cells cycled to UCV of 4.2 V, where performance differences were relatively minor between the two formulations. Linear sweep voltammetry (**Figure S7**) accounts for this difference as a reduced oxidative stability of LP57 containing 2 wt.% VC at *ca.* 4.4 V is observed.

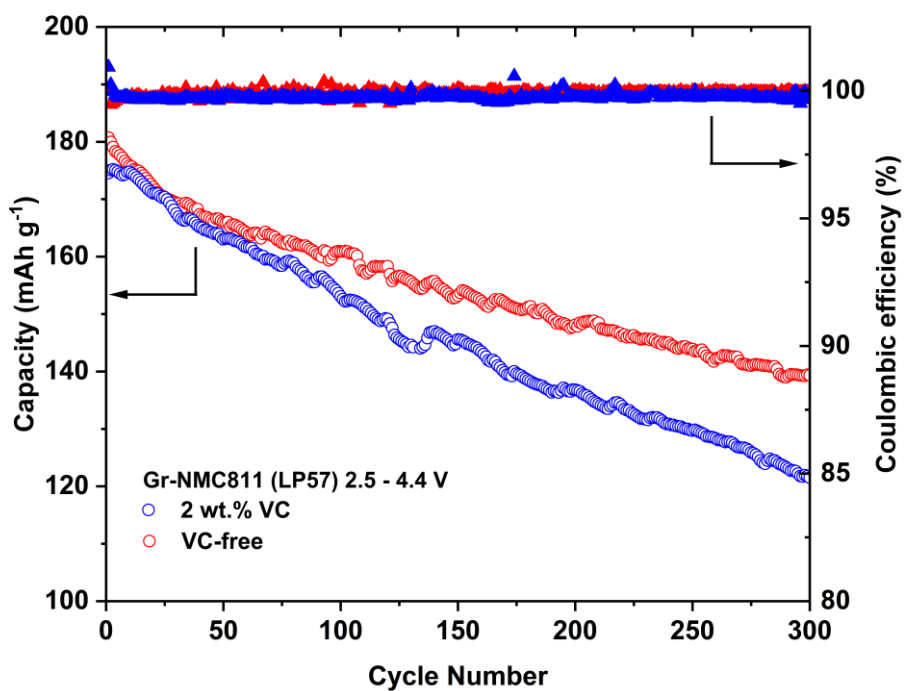


Figure S6. Cycling data for Gr-NMC811 full-cells showing that addition of 2 wt.% vinylene carbonate results in worse cell performance when cycled to an UCV of 4.4 V at a rate of 1C.

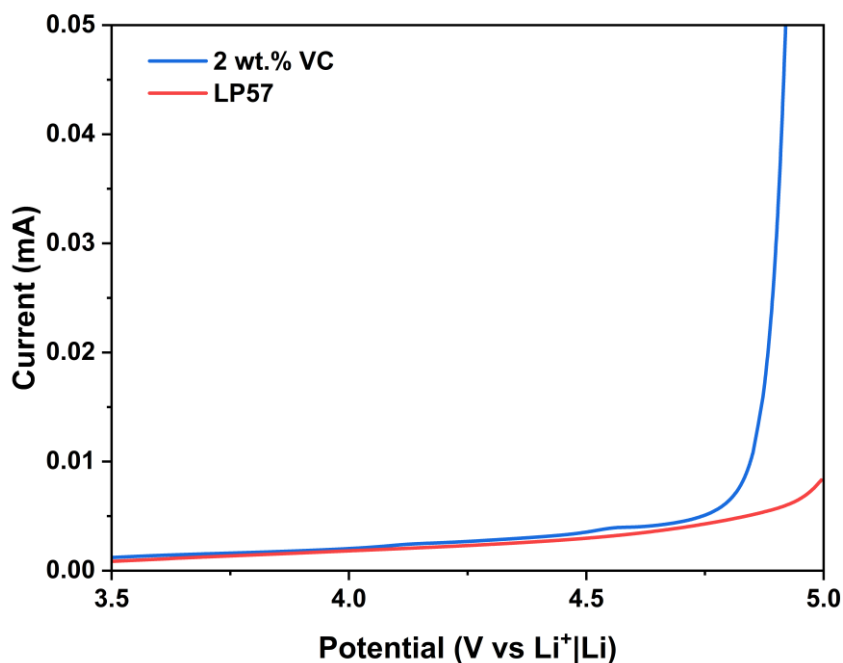


Figure S7. Linear sweep voltammograms of LP57 and LP57 + 2 wt.% VC at a glassy carbon electrode depicting their respective oxidative stabilities. A small peak at around 4.5 V vs $\text{Li}^+|\text{Li}$, or ca. 4.4 V corrected to Gr-NMC811, is observed when VC is present.

Online mass spectrometry (OMS) for monitoring singlet oxygen reactivity. OMS experiments were carried out using equipment designed and produced by the NAMI group and the University of Nottingham Mechanical Workshop. These design were based on original reports by Tsiouvaras and co-workers,⁵ and fitted with an Hiden Analytical quadrupole mass spectrometer.

General procedure A: In an N₂-filled glovebox, a vacuum dried microwave vial fitted with a PTFE stirrer bar was charged with DMA (4.6 mg, 22 μmol) if using, EC stock solution of photocatalyst (RB or TPP), and then diluted further with EC to a 10 μM photocatalyst solution (final volume: 2 mL). The vial was sealed with a septum-lined cap and connected to the OMS, temperature held at ca. 40 °C while stirring, and headspace purged (>6 h) with a 20 % O₂ in Ar until steady baselines of O₂ (*m/z* = 32) and CO₂ (*m/z* = 44) at 0.2 ml min⁻¹ were achieved. Samples were irradiated for 110 minutes by a green LED lamp (5 W) for RB or a Kessil Tuna Flora H160 (40W) lamp set to red (100% intensity) for TPP, upon removal of the light, gas monitoring continued until a new baseline was met.

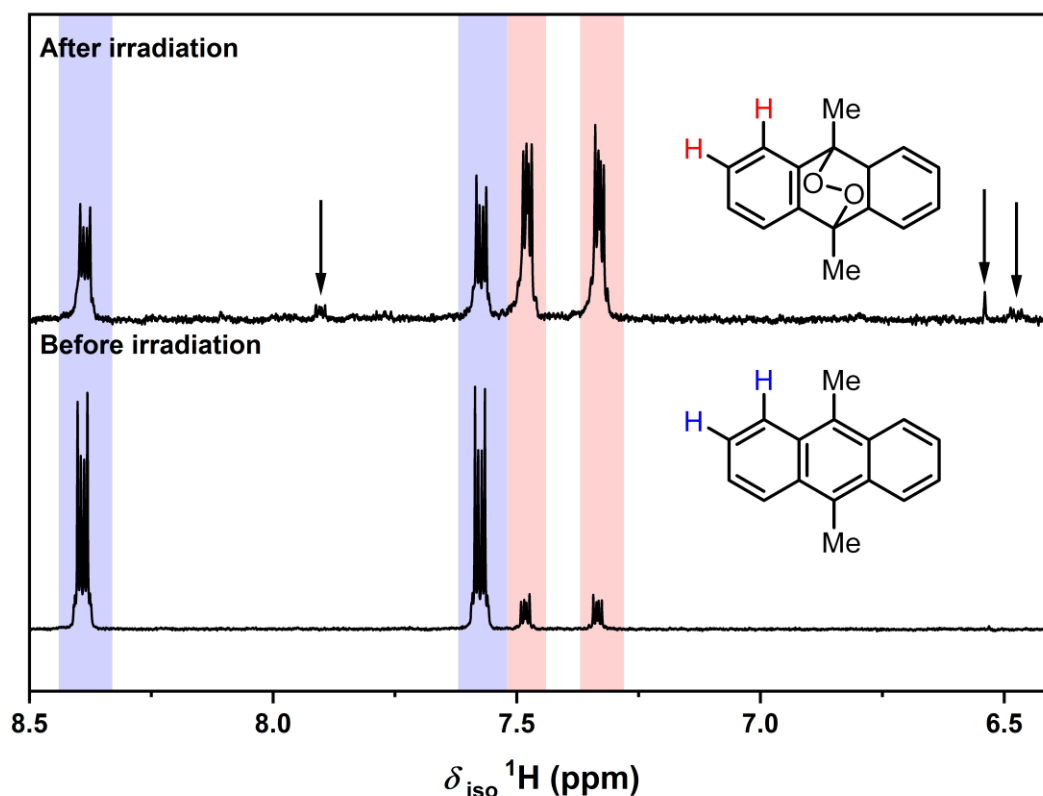


Figure S8. ¹H NMR spectra (500 MHz, DMSO-d₆) of an aliquot from the OMS experiment of DMA in EC with 10 μM RB before and after irradiation by green light. The aromatic protons signals for DMA (blue) and DMA-O₂ (red) are depicted. Arrows highlight by-product peaks. Trimethoxy benzene was included as an internal standard for determining selectivity (resonances not shown).

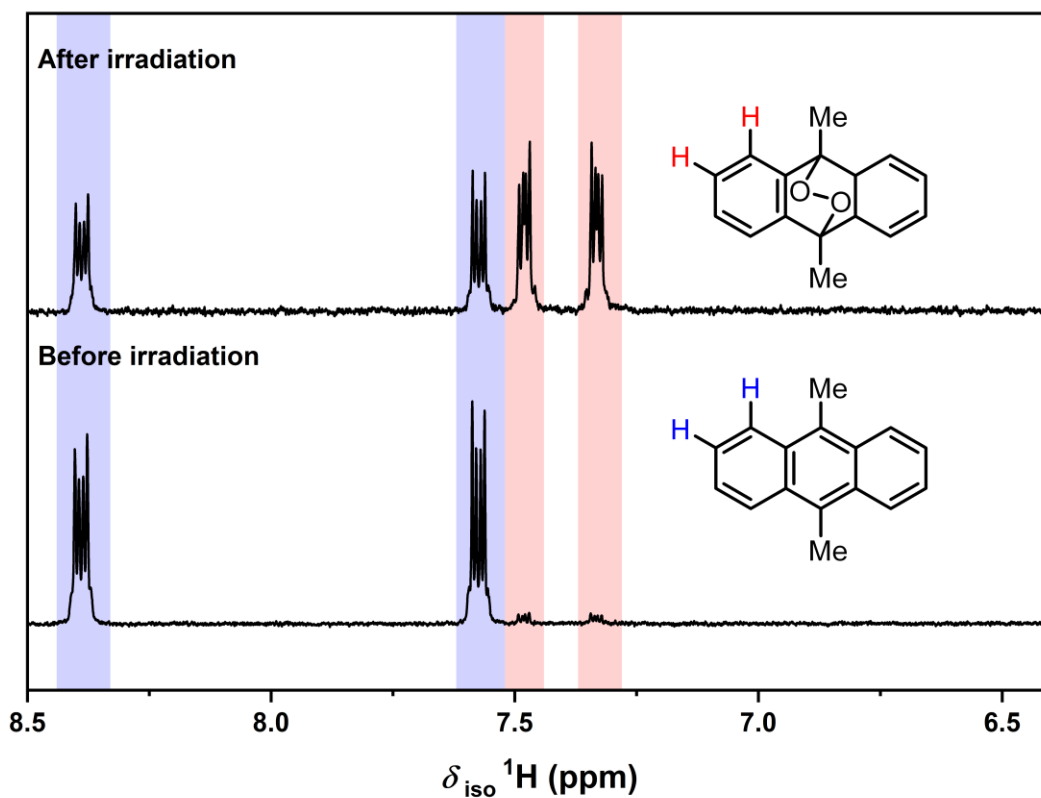


Figure S9. ¹H NMR spectra (500 MHz, DMSO-d₆) of aliquots from the OMS experiment of DMA in EC with 10 μM TPP before and after irradiation by red light. The aromatic protons signals for DMA (blue) and DMA-O₂ (red) are depicted. Trimethoxy benzene was included as an internal standard for determining selectivity (resonances not shown).

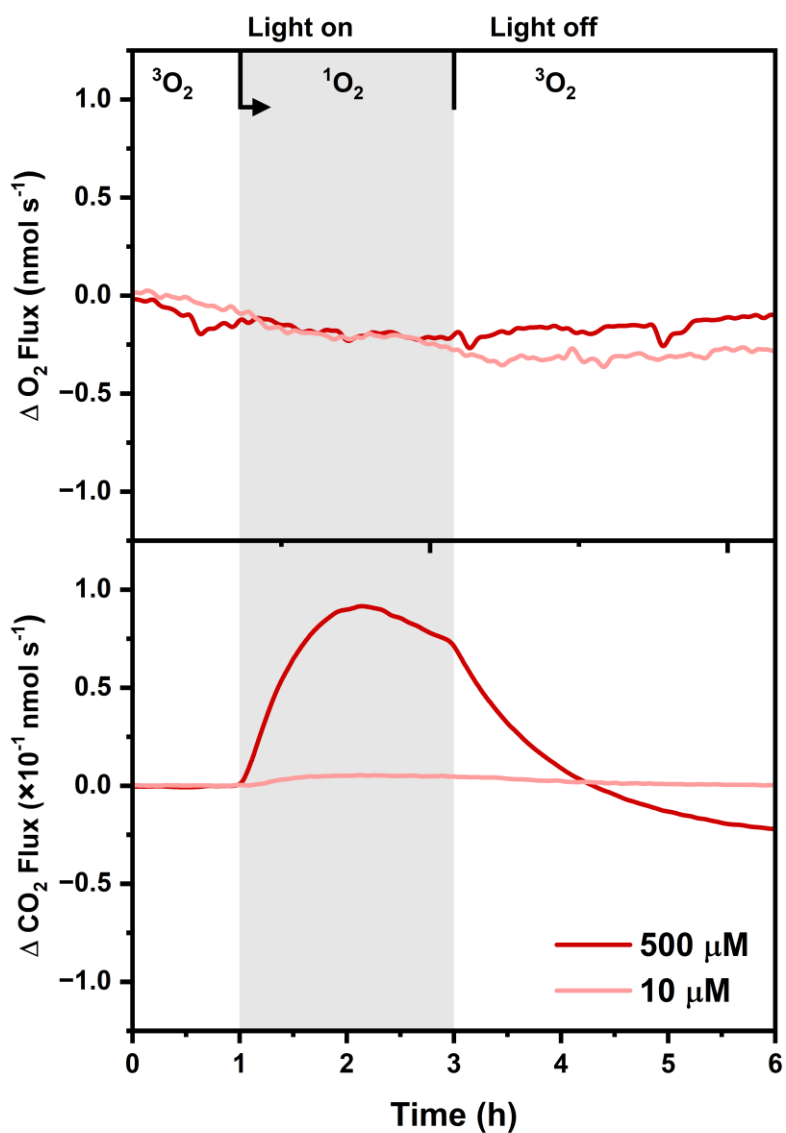


Figure S10. Overlaid OMS data showing O_2 and CO_2 flux when 10 μM or 500 μM RB in EC is irradiated with a green LED lamp according to general procedure A.

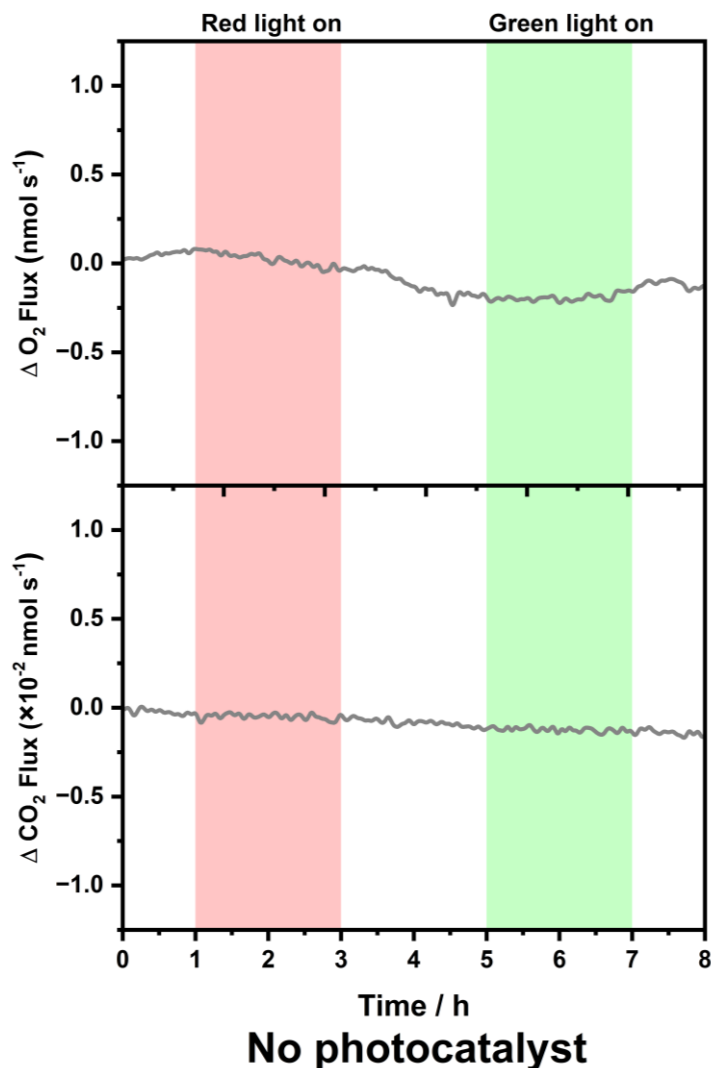


Figure S11. OMS data showing no significant change in CO₂ and O₂ flux when EC is irradiated without the presence of a photocatalyst (20% O₂ in Ar, 0.2 ml min⁻¹).

Rationale for RB coupled CO₂ generation: Photobleaching of RB in EC is observed (**Figure S12**, left) after 110 minutes of illumination under oxygenated conditions during OMS experiments conducted according to general procedure A. Photochemical reaction mechanisms for the xanthene class of photocatalysts is well described in literature,⁶ which account for photobleaching. To summarise, following photoexcitation, charge transfer reactions generating reactive RB radical ions can occur.⁶ These reactive radical ions undergo secondary reactions with components (photocatalyst, solvent, substrates etc), resulting in irreversible changes to the photocatalyst structure. In the case of RB, one photodegradation route coincides with CO₂ release due to decarboxylation of the CO₂⁻ moiety (**Figure S12**, right). While photobleaching of TPP also occurs slowly under these conditions (**Figure S15**), no sensible decarboxylative pathway based on its structure is evident, hence CO₂ release is not observed for TPP.

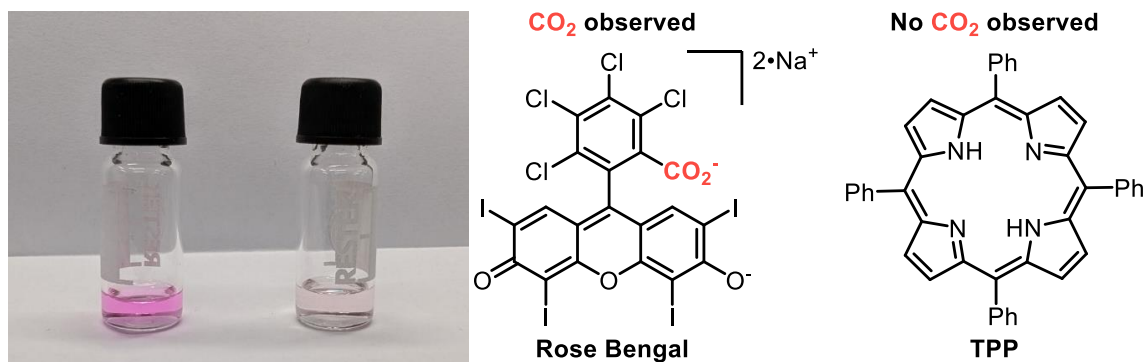
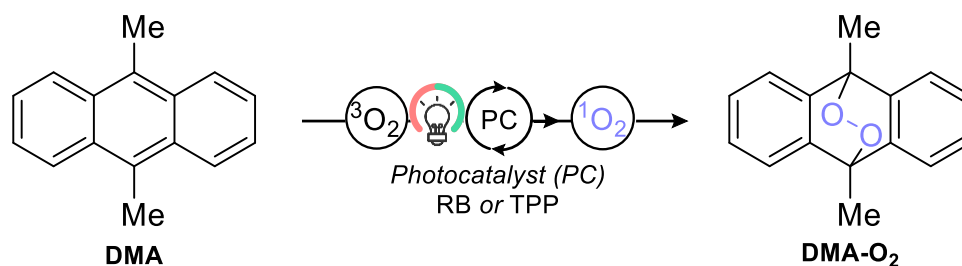


Figure S12. Image of 10 μM RB in EC before and after 110 mins of illumination under atmosphere of O₂ demonstrating catalyst bleaching (left). Structures of rose bengal and TPP (right).

Estimation of ¹O₂ production: By assuming the cycloaddition reaction between ¹O₂ and DMA to yield DMA-O₂ is directly proportional to ¹O₂ formation (**Scheme S1**), *i.e.* 100% capture rate, the approximate rate and moles of ¹O₂ produced under specified reaction conditions can be calculated. This is likely an underestimate.



Scheme S1. Photocatalytic generation of ¹O₂ for reaction with DMA.

Photogeneration of ¹O₂ in EC with DMA following general procedure A resulted in reduction in O₂ flux during illumination indicating ¹O₂ generation and subsequent reaction with DMA. By integration (**Figure S13**), approximately 5.6 μmol (0.85 nmol s^{-1}) and 10.7 μmol (1.6 nmol s^{-1}) of ¹O₂ was captured for reactions using 10 μM RB or TPP, respectively.

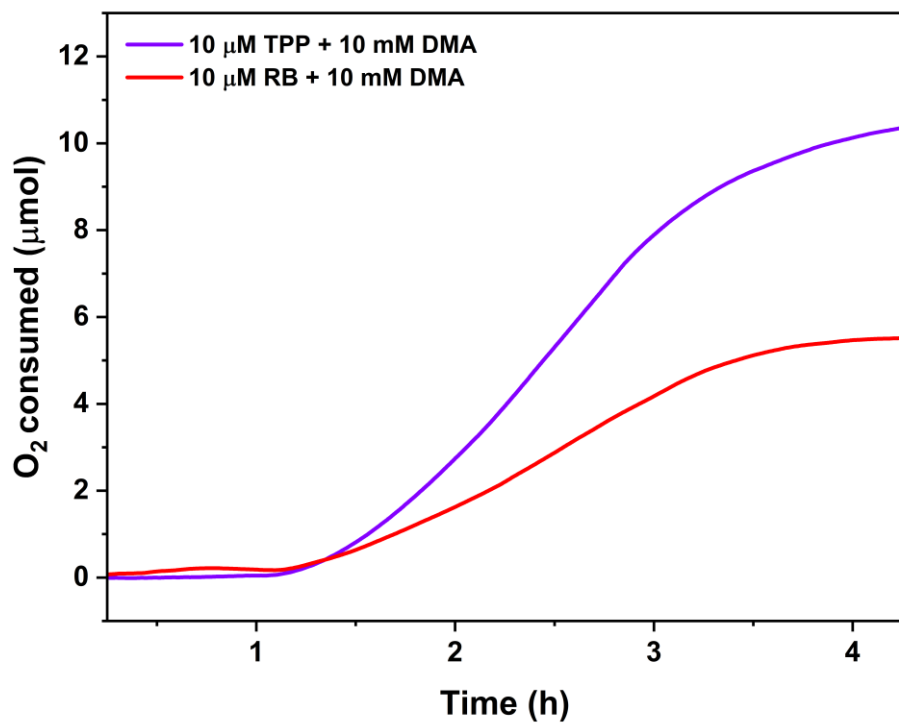


Figure S13. O₂ flux integration versus time obtained from OMS when an EC solution containing 10 mM DMA with 10 μM TPP (purple) or 10 μM RB (red) was irradiated.

Supplementary Note 2 – Extended exposure study of EC to $^1\text{O}_2$

DMA oxidation by $^1\text{O}_2$ in CDCl_3 : A microwave vial fitted with a PTFE stirrer bar was charged with a stock solution of TPP (1.1 mM in CH_2Cl_2 , 0.45 mL), CH_2Cl_2 removed *in vacuo* before addition of DMA (103 mg, 0.50 mmol, 0.1 M), trimethoxybenzene (21.6 mg, 0.125 mmol, 0.025M), and CDCl_3 (5 mL). The vial was sealed with a septum-lined cap and sparged with O_2 (balloon) for 5 min before illumination by a Kessil Tuna Flora H160 (40W) lamp set to red (100% intensity) while stirring at room temperature. Aliquots were taken under an atmosphere of O_2 (balloon) for analysis by ^1H NMR spectroscopy, the solution was then sparged with O_2 for ~2 min before reilluminating.

Complete conversion of DMA to DMA- O_2 (with 99% selectivity) was observed within 2 hours of irradiation under these 100 μM TPP reaction conditions (**Figure S14**). The amount $^1\text{O}_2$ capture by DMA was determined to be 0.49 mmol (69 nmol s^{-1}) by ^1H NMR spectroscopy. The estimated amount of $^1\text{O}_2$ generation under these conditions is approximately 40 times greater than that in the OMS experiments (**Figure S13**).

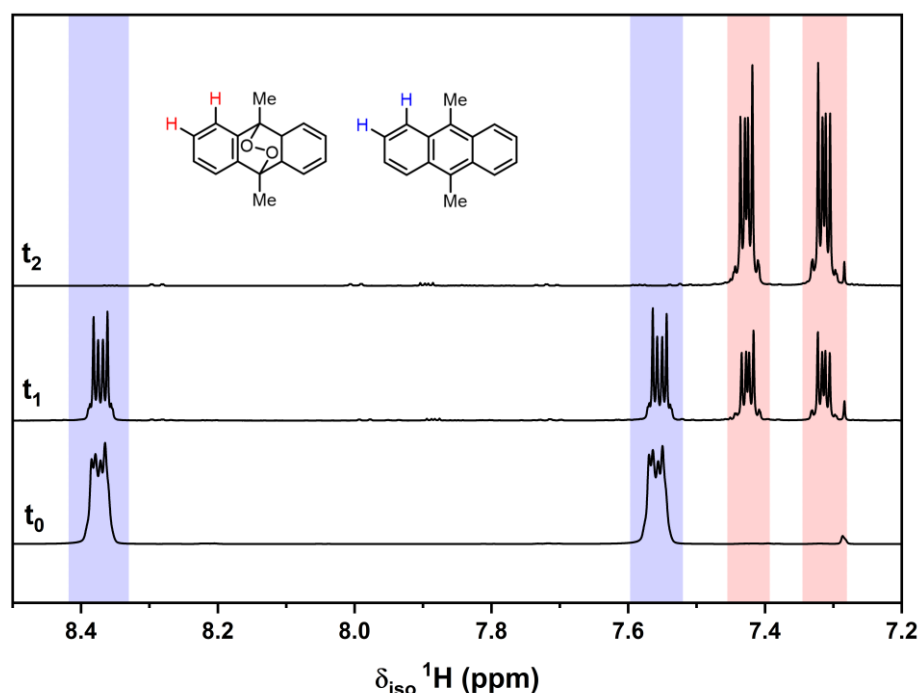


Figure S14. ^1H NMR spectra (500 MHz, CDCl_3) showing complete conversion of DMA to DMA- O_2 by $^1\text{O}_2$ within 2 h using 100 μM TPP in CDCl_3 . Trimethylbenzene (0.025 M) was used as an internal standard (resonances not shown).

Quantitative ^1H NMR spectroscopic details: T1 values for ethylene carbonate (0.1 M) and dimethyl sulfone (0.0125 M) in CDCl_3 were determined by inversion-recovery experiments on a Bruker AV(III)500 HD fitted with a 5 mm prodigy BBO cryoprobe. The data was processed using Bruker's Topspin software. The T1 values for EC (4.52 ppm, s, 4H, $2\times\text{CH}_2$) and dimethylsulfone (2.98 ppm, 6H, s, $2\times\text{CH}_3$) under these conditions were calculated to be 3.99 s and 5.74 s, respectively. The size of fid (TD), transmitter frequency

(O1P) and spectral width (SW) were set to 65536, 5 ppm and 10 ppm, respectively, resulting in a 6.55 sec acquisition time.

Quantitative ^1H NMR spectroscopic monitoring consumption of EC by $^1\text{O}_2$: A microwave vial fitted with a PTFE stirrer bar was charged with a stock solution of TPP (1.1 mM in CH_2Cl_2 , 0.45 mL), CH_2Cl_2 removed *in vacuo* before addition of EC (44 mg, 0.50 mmol, 0.1 M), dimethyl sulfone (11.9 mg, 0.125 mmol, 0.025M), and CDCl_3 (5 mL). The vial was sealed with a septum-lined cap and sparged with O_2 (balloon) for 5 min before illumination by a Kessil Tuna Flora H160 (40W) lamp set to red (100% intensity) while stirring at room temperature. Aliquots were taken under an atmosphere of O_2 (balloon) for analysis by ^1H NMR spectroscopy, the solution was then sparged with O_2 for ~2 min before reilluminating. Reactions were conducted in duplicate with inclusion of an internal standard to reduce systematic error.

Photocatalyst stability: By ^1H NMR spectroscopy, photobleaching of 100 μM TPP in a solution of 0.1 M EC in CDCl_3 occurs slowly over 22 h with retention of the photoactive structure up to at least 8 h of irradiation (**Figure S15**), suggesting that EC was continually exposed to singlet oxygen for at least 4 times that of the OMS experiments.

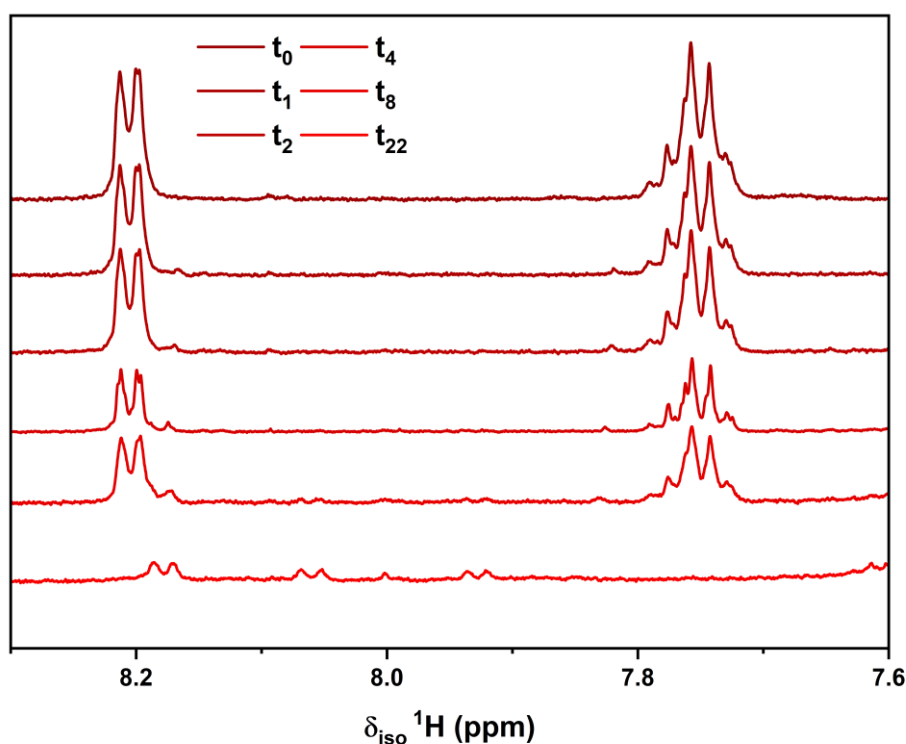


Figure S15. ^1H NMR spectra (500 MHz, CDCl_3) showing stability of TPP over time while illuminated. The active porphyrin core remains present up to 8 h, with complete photo bleaching occurring by 22 h. Intensities normalised to internal standard.

References

1. G. R. Fulmer, A. J. M. Miller, N. H. Sherden, H. E. Gottlieb, A. Nudelman, B. M. Stoltz, J. E. Bercaw and K. I. Goldberg, *Organometallics*, 2010, **29**, 2176–2179.
2. L. M. Thompson, W. Stone, A. Eldesoky, N. K. Smith, C. R. M. McFarlane, J. S. Kim, M. B. Johnson, R. Petibon and J. R. Dahn, *J. Electrochem. Soc.*, 2018, **165**, A2732.
3. Mass Spectrometry Data Center, NIST, <https://chemdata.nist.gov/>.
4. D. A. Armbruster, M. D. Tillman and L. M. Hubbs, *Clin. Chem.*, 1994, **40**, 1233–1238.
5. N. Tsiouvaras, S. Meini, I. Buchberger and H. A. Gasteiger, *J. Electrochem. Soc.*, 2013, **160**, A471.
6. N. A. Romero and D. A. Nicewicz, *Chem. Rev.*, 2016, **116**, 10075–10166.